Surface Catalytic Reactions Assisted by Gas Phase Molecules

YASUHIRO IWASAWA*

Department of Chemistry, Graduate School of Science, The University of Tokyo, Hongo, Bunkyo-ku, Tokyo 113, Japan

Received July 11, 1995

Introduction

Selectivity in catalytic oxidation and acid−base reactions has been a long-term challenge in the field of oxide surface chemistry. While it has been recognized that control of activation and reaction intermediates is critical in achieving selectivity, this issue has not been adequately addressed and is a serious challenge to the field.

The aim of this Account is to illustrate how weakly adsorbed molecules can promote catalytic reactions. *Weakly adsorbed molecules at catalyst surfaces can exist only under catalytic reaction conditions in the presence of gas phase molecules*. Recently, it has been demonstrated that weakly adsorbed molecules can activate the reaction of strongly-adsorbed intermediates, ultimately controlling the catalytic reaction path.[1,2] In this Account two typical examples of reactions are presented, i.e., the ethanol dehydrogenation on one-component designed Nb mono-

mers supported on SiO_2 and the water−gas shift reaction on basic metal oxide catalysts.

A simplified form of the usual mechanism for heterogeneous catalytic reactions is shown in Figure 1a, where the reaction intermediate (**X**) is transformed to the product (**P**) by surface unimolecular decomposition; that is, a stoichiometric reaction step proceeds without aid of other molecules. In a typical catalyst, a role of the active site is to directly activate the adsorbed intermediate, which makes it possible for the bond rearrangement to occur in a desired manner. A typical example is seen for ethanol oxidation on molybdenum oxide catalysts, where the molybdenum ethoxide intermediate ($Mo−OC_2H_5$) at the surface decomposes by itself to a product, acetaldehyde, and the behavior of the intermediate is similar under vacuum and catalytic reaction conditions when the surface coverage (equivalent to concentration) is identical under both atmospheres. Similarly, the water−gas shift (WGS) reaction, $H_2O + CO \rightarrow H_2 + CO_2$, has been believed to proceed via surface formate ions ($HCOO^-$) as the reaction intermediate (**X**), involving bond rearrangement. The feature would also be valid for the Langmuir−Hinshelwood mechanism, e.g., $CO + {}^1/_2O_2 \rightarrow CO_2$, in which two adsorbed species (CO(a) and O(a)) independently interact with the surface sites and subsequently react with each other. The surface reaction requires no additional gas phase molecules.

In contrast to the simple expectation of no special role of additional gas phase molecules in a catalytic mechanism, we have found evidence that the reaction intermediate of an important catalytic reaction can be profoundly influenced by the ambient gas. In particular, the reaction involved the new SiO_2-supported niobium monomer catalyst which was the first to be active for dehydrogenation of ethanol, $C_2H_5OH \rightarrow CH_3CHO + H_2$.[3] Niobium

* Fax: 81-3-5800-6892. E-mail: iwasawa@utsc.s.u-tokyo.ac.jp.
(1) Iwasawa, Y. The Effects of Coadsorbates on the Behaviour of Surface Species and Sites in Catalysis by Means of EXAFS and FT-IR. In *Elementary Reaction Steps in Heterogeneous Catalysis*; Joyner, R. W., van Santen, R. A., Eds.; NATO ASI Series C; Kluwer: Dordrecht, The Netherlands, 1993; Vol. 398, p 287.
(2) Iwasawa, Y. *Proceedings of the 11th International Congress on Catalysis*, Baltimore; Hightower, J. W., Delgass, W. N., Iglesia, E., Bell, A. T., Eds.; Elsevier: Amsterdam, The Netherlands, 1996; p 21.
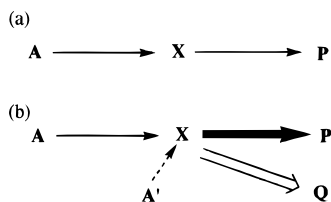(3) Nishimura, M.; Asakura, K.; Iwasawa, Y. *J. Chem. Soc., Chem. Commun.* **1986**, 1660.

FIGURE 1. (a) Surface catalytic reaction (A → P) via intermediate X. (b) Surface catalytic reaction (A → P) promoted by reactant molecule A′, where enhancement of the reaction rate for the formation of P or switchover of the reaction path from P formation to Q formation is by reactant molecule A′.

has recently attracted much attention as a key element for industrially important processes such as ammoxidation of propane,[4] oxidative dehydrogenation of propane,[5] and liquid phase catalysis.[6] In the catalytic dehydrogenation reaction of ethanol on the Nb monomer catalyst the intermediate (**X**) was stable and did not decompose to a product (**P**) up to 600 K, whereas in the coexistence of another reactant molecule (**A′**) the intermediate (**X**) is activated to decompose to a different product (**Q**) even at low temperatures like 473 K (Figure 1b). Enhancement of the rate of the intermediate decomposition and switchover of the reaction path in Figure 1b were also found in water−gas shift reactions on MgO, ZnO, and Rh/CeO$_2$ as described below.

This Account emphasizes a novel issue in catalysis, namely, that surface catalytic reaction pathways are made accessible by ambient gas phase molecules that are weakly adsorbed. In particular, the paper is concerned with the catalytic role of weakly adsorbed molecules that participate as "promoters" in the catalytic pathway, but are undetectable. The issues that are addressed in this Account are generally relevant to catalytic systems. Furthermore, they suggest new strategies for development of catalytic materials and systems.

Ethanol Dehydrogenation Promoted by Weakly Adsorbed Ethanol on Nb Monomers

Preparation and Characterization of Nb Monomers on SiO$_2$. The supported Nb monomer catalyst (**1**) in Scheme 1 was prepared via the surface complex which was obtained by reaction between Nb (η^3-C$_3$H$_5$)$_4$ and surface OH groups of SiO$_2$ (Aerosil 200; pretreated at 673 K) at 233−273 K, followed by treatments with H$_2$ and O$_2$.[3,7] The surface complexes were successively reduced with H$_2$ and oxidized with O$_2$ at 673 K to obtain the Nb^{5+} state (**1**). The Nb^{5+} state was confirmed by the Nb 3d$_{3/2}$ and 3d$_{5/2}$ binding energies of the catalyst (**1**). The X-ray absorption near-edge structure (XANES) spectrum exhibited a distinct peak assignable to the 1s → 4d transition for Nb^{5+} ions of a four-coordinated structure rather than octahedral symmetry. The Nb−O, Nb=O, and Nb−Si interatomic distances in the structure (**1**) were determined to be 0.193, 0.168, and 0.326 nm, respectively, by a curve-fitting analysis of the Nb K-edge EXAFS data as shown in Scheme
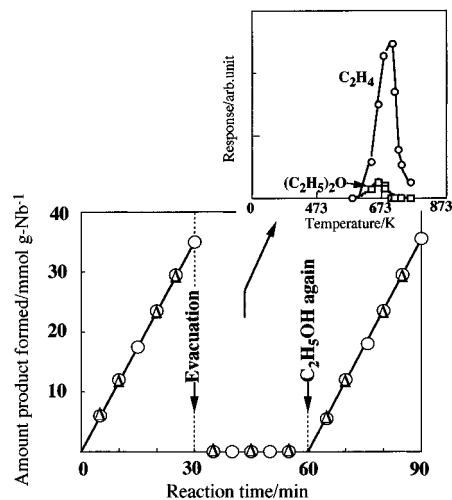
(4) Ushikubo, T.; et al. (Mitsubishi Kasei Corp.). Jpn. Tokkai, H5-208136; H6-116225.
(5) Smits, R. H. H.; Seshan, K.; Ross, J. R. H. *ACS Prepr. Pet. Div.* **1992**, *37*, 1121.
(6) Ushikubo, T.; Hara, Y.; Wada, K. *Catal. Today* **1993**, *16*, 525.
(7) Nishimura, M.; Asakura, K.; Iwasawa, Y. *Chem. Lett.* **1986**, 1457.

FIGURE 2. Ethanol dehydrogenation on Nb/SiO$_2$ (○, H$_2$; △, CH$_3$CHO) and TPD spectrum of adsorbed ethanol (species 2). Heating rate 4 K min^{-1}.

Scheme 1. Switchover of the Reaction Paths by Gas Phase Ethanol
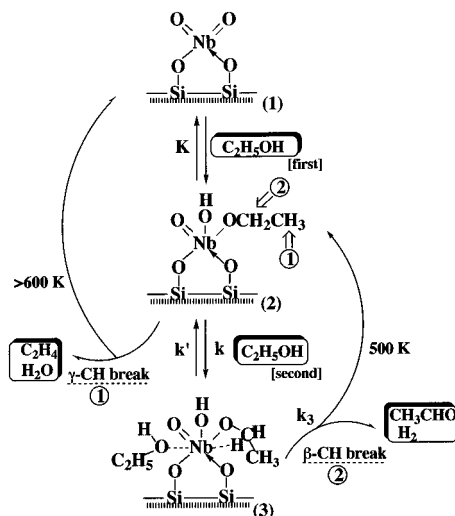
1. No Nb−Nb bonding was observed by EXAFS, demonstrating that the Nb^{5+} ions in the catalyst (**1**) are distributed as isolated species (monomers).[3,8]

Mechanism for Catalytic Dehydrogenation of Ethanol. The SiO$_2$-supported Nb catalyst (**1**), {SiO}$_2$Nb(=O)$_2$, exhibits a high activity and selectivity for the dehydrogenation reaction. Acetaldehyde and hydrogen were stoichiometrically produced during the catalytic reaction as shown in Figure 2. Ethanol dissociatively adsorbs on Nb to form C$_2$H$_5$O(a) and OH(a), {SiO}$_2$Nb(=O)(OH)(OC$_2$H$_5$) (**2**) in Scheme 1. This is proved by IR spectra using C$_2$H$_5$-OH, C$_2$H$_5$OD, and C$_2$D$_5$OH. The IR spectra exhibit the ν_{OH} peak at 3440 cm^{-1} for Nb−OH and the ν_{CH} peaks at 2979, 2935, 2900, and 2885 cm^{-1} for Nb−OC$_2$H$_5$ in the case of C$_2$H$_5$OH, the ν_{OD} peak at 2577 cm^{-1} for Nb−OD and the ν_{CH} peaks at 2979, 2935, 2900, and 2885 cm^{-1} for Nb−OC$_2$H$_5$ in the case of C$_2$H$_5$OD, and the ν_{OH} peak at 3440 cm^{-1} for Nb−OH and the ν_{CD} peaks of 2229, 2139, and 2090 cm^{-1} for Nb−OC$_2$D$_5$ in the case of C$_2$D$_5$OH. The ν_{OH} peak and the ν_{CH} peaks for adsorbed C$_2$H$_5$OH are replaced by the ν_{OD} peak or the ν_{CD} peaks by C$_2$H$_5$OD or C$_2$D$_5$OH

(8) Nishimura, M.; Asakura, K.; Iwasawa, Y. *Proc. 8th Int. Congr. Catal. Calgary* **1988**, *4*, 1566.

adsorption, respectively. The adsorbed species OH(a) and $C_2H_5O(a)$ are stable in vacuum, while the exchange reaction with the gas phase ethanol readily occurs.[8] The ν_{OH} peak and the ν_{CH} peaks are only observed peaks under the catalytic C_2H_5OH dehydrogenation reaction conditions.

When the gas phase ethanol was evacuated in the course of the dehydrogenation at 523 K, the reaction completely stopped as shown in Figure 2. However, the amount of adsorbed ethanol, $\{SiO\}_2Nb(=O)(OH)(OC_2H_5)$ (**2**), remained unchanged by the evacuation as evidenced by the intensity of the ν_{OH} and ν_{CH} peaks. In other words, the adsorbed ethanol was converted selectively to acetaldehyde and hydrogen under the ambient ethanol at 423–523 K, whereas the adsorbed ethanol was never decomposed under vacuum in the same temperature range.[8] This might be a strange aspect in a sense because the ethanol dehydrogenation has been thought to be a surface reaction which proceeds via decomposition of the adsorbed ethanol, the rate of which depends only on the coverage of the adsorbed ethanol, not on the pressure of gas phase molecules. To gain insight into the reactivity of adsorbed ethanol, a temperature-programmed desorption (TPD) spectrum for $\{SiO\}_2Nb(=O)(OH)(OC_2H_5)$ (**2**) formed during the catalytic ethanol dehydrogenation reaction was measured as shown in Figure 2 (inset), which revealed that the reaction of adsorbed ethanol (**2**) in vacuum was only possible at higher temperatures than 600 K, with a TPD peak at 700 K. The TPD peak is observed in a much higher temperature range than 423–523 K for the catalytic reactions, and the TPD products are ethene and water (dehydrated products), in contrast to acetaldehyde and hydrogen (dehydrogenated products) produced in the catalytic reactions. *Note that the behavior of adsorbed ethanol (2) is entirely different in vacuum and in the presence of ambient ethanol.* The dehydrogenation reaction started again by introducing ethanol vapor onto adsorbed ethanol (**2**) as shown in Figure 2. Thus, it seems that the catalytic dehydrogenation reaction is assisted by the ambient ethanol, where the reaction path of adsorbed ethanol (**2**) is switched from dehydration to dehydrogenation by the ambient ethanol. In other words, adsorbed ethanol (**2**) prefers the dehydration to form ethene and water by *the γ-hydrogen abstraction*, while in the presence of the ambient ethanol *the β-hydrogen abstraction* from adsorbed ethanol (**2**) to form acetaldehyde and hydrogen dominates as shown in Scheme 1. To examine how and why the surface ethanol reaction is assisted by the gas-phase ethanol, the following experiments were conducted in a closed circulating reactor.

Ethanol vapor was first admitted onto the dioxonio-bium monomer catalyst (**1**), $\{SiO\}_2Nb(=O)_2$, to form the niobium ethoxide (**2**), $\{SiO\}_2Nb(=O)(OH)(OC_2H_5)$, at 373 K, followed by evacuation, and then the system was maintained at 523 K for 10 min, where no H_2 evolution was observed because the niobium ethoxide (**2**) was stable up to 600 K in vacuum. After the confirmation of no H_2 formation from the preadsorbed ethanol (**2**), *tert*-butyl alcohol was introduced to the system at 523 K, which led to a stoichiometric evolution of H_2 and CH_3CHO. As the *tert*-butyl alcohol molecule has no extractable α-hydrogen,
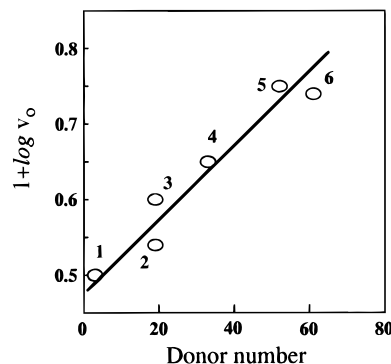

FIGURE 3. Correlation between the initial rate of CH_3CHO (H_2) formation from species 2 and the donor number of nucleophilic compounds (1, CH_3NO_2; 2, $(C_2H_5)_2O$; 3, THF; 4, C_5H_5N; 5, $C_5H_{11}N$; 6, $(C_2H_5)_3N$).

it is evident that both H_2 and CH_3CHO were produced from the preadsorbed ethanol by the assistance of the postdosed *tert*-butyl alcohol.

To confirm this mechanistic feature and to examine the interaction between the niobium ethoxide species and the postadsorbed molecule, various electron-donating compounds were postadsorbed on the surfaces preadsorbed with the same amount of ethanol, $\{SiO\}_2Nb(=O)-(OH)(OC_2H_5)$ (**2**). Equimolar amounts of H_2 and CH_3CHO were produced from the preadsorbed ethanol (**2**) by admission of the electron donors. The logarithm of the initial rates of the CH_3CHO (H_2) formation from the preadsorbed ethanol (**2**) was plotted against the donor number of the postadsorbed molecules which undissociatively (molecularly) adsorb on the Nb atom as shown in Figure 3, where the donor number is defined as the logarithm of the equilibrium constant for the formation of electron donor–acceptor complexes between the nucleophilic molecules and $SbCl_5$ and regarded as the electron donor strength of the postadsorbed molecules. The linear relationship that is shown in Figure 3 indicates that the electron donor–acceptor interaction between the postadsorbed molecule and the coordinatively unsaturated Nb d^0 ion is a key issue for the dehydrogenation of the preadsorbed ethanol (**2**).[8]

Accordingly, the catalytic dehydrogenation reaction of ethanol is likely to proceed via species (**3**) involving a second (postadsorbed) ethanol molecule as shown in Scheme 1. In fact, when $\{SiO\}_2Nb(=O)(OH)(OC_2H_5)$ (**2**) was exposed to C_2D_5OD, H_2 was first produced, followed by HD formation, and then D_2 formation was observed in the time profile for the product. HD is produced from $\{SiO\}_2Nb(=O)(OC_2H_5)$ which is formed by rapid hydroxyl exchange of OH(a) with C_2D_5OD, and D_2 is produced from $\{SiO\}_2Nb(=O)(OD)(OC_2D_5)$ which is formed by ligand exchange of both OH(a) and $C_2H_5O(a)$ with C_2D_5OD as proved by FT-IR. This profile for the hydrogen formation as a function of reaction time demonstrates that the postadsorbed ethanol promotes the dehydrogenation of the preadsorbed ethanol in a manner similar to that of the electron-donating molecules in Figure 3. The mechanism is shown in Scheme 1.

The weakly adsorbed ethanol (postadsorbed ethanol) (**3**) present only under the catalytic reaction conditions in Scheme 1 was kinetically characterized as follows. The formation of the surface species (**2**) in Scheme 1 was

Table 1. IR Bands of ν_{as}(OCO) and ν_s(OCO) for the Formates and the Rate Constants, k_+ and k_-, of the Forward and Backward Decompositions of the Formates, Respectively, on MgO in the Absence and the Presence of Electron-Donating Molecules[a]

molecule	ν(CD)/ cm^{-1}	ν_{as}(OCO)/ cm^{-1}	ν_s(OCO)/ cm^{-1}	k_+/ $(10^{-4}$ s$^{-1})$	k_-/ $(10^{-4}$ s$^{-1})$
none (vacuum)	2120	1615	1321	0	13
water	2130	1593	1333	1.4	0.5
methanol	2125	1600	1334	0.5	7
pyridine	2121	1595	1334	0	12
THF	2120	1610	1330	0	13

[a] Rate constants were measured at 600 K.

nearly saturated at the ethanol pressure of 2.4 kPa as proved by FT-IR, but the reaction rate increased over its pressure and saturated at 3.7 kPa of ethanol. Adsorption of ethanol measured by volumetry, taking into account the adsorption on SiO$_2$, showed the tendency of saturation around 2.4 kPa of ethanol, but increased up to 3.7 kPa. The saturation of the rate coincides well with that of the catalytic reaction rate saturated at 3.7 kPa. Thus, further adsorption of ethanol on species **2** may be suggested as shown in Scheme 1. Assuming the mechanism in Scheme 1, the following equation is derived from a steady-state procedure:

$$\frac{[Nb]_o}{v} = \frac{1}{k_3} + \frac{k' + k_3}{kk_3}\frac{KP + 1}{KP^2}$$

where v, $[Nb]_o$, and P represent the reaction rate, the amount of Nb sites, and the ethanol pressure, respectively. Plots of $[Nb]_o/v$ against $(KP + 1)/KP^2$ showed a linear relationship, suggesting the validity of the mechanism in Scheme 1.[8] Further, the mechanism was also supported by the fact that the rate constant k_3 (1.5 mmol min^{-1} (g of Nb)$^{-1}$) determined from the steady-state equation was almost the same as the value of k_3 determined from the initial rate of the dehydrogenation of species **3** under the condition of ethanol adsorbed at saturation. The equilibrium constant for weak adsorption of ethanol, k/k', was calculated to be 9.0×10^{-4} Pa^{-1}. The weakly adsorbed ethanol is in equilibrium with the gas phase ethanol, and easily desorbs from the surface in vacuum.

The dehydrogenation mechanism in Scheme 1 reveals the switchover of the reaction path from dehydration (γ-CH bond break) to dehydrogenation (β-CH bond break) by whether or not ethanol molecules are present in the gas phase. For this reaction, the adsorbed species are stable in vacuum. In the presence of additional gas phase molecules, the catalytic reaction is able to proceed; in other words, this is a reactant-promoted mechanism.[3,8] Thus, the presence of a vacant site with an appropriate conformation on the Nb site may be critical in opening a dehydrogenation path.

Behavior of the Surface Reaction Intermediate under the Ambient Molecules in the Water−Gas Shift Reaction
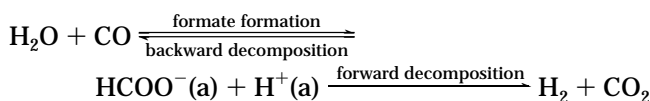
The water−gas shift (WGS) reaction on MgO, ZnO, and Rh/CeO$_2$ is another example of a surface catalytic reaction that is assisted by gas phase molecules. The behavior of surface formate intermediates (HCOO$^-$) is remarkably influenced by weakly coadsorbed water molecules.

WGS Reaction on the MgO Surface. Water dissociatively adsorbs to form OH groups on many oxide surfaces. The local structures of OH groups on MgO have been characterized in detail by FT-IR.[9] There are three kinds of linear OH groups on Mg atoms with the different coordination of O atoms, Mg$_{5c}$, Mg$_{4c}$, and Mg$_{3c}$ (c = coordinatively unsaturated site), and three kinds of bridge OH groups with different coordination of Mg atoms, O$_{3c}$, O$_{4c}$, and O$_{5c}$. Only linear OH groups on Mg$_{3c}$ and Mg$_{4c}$ among the linear and bridge OH groups react with CO to form surface formates at 600 K as proved by FT-IR. The structure of the formates thus formed (unidentate, bidentate, or bridge types) can be determined by the value of $\Delta\nu = \nu_{as}$(OCO) $- \nu_s$(OCO).[10] When $\Delta\nu$ is larger or smaller than that of a free ion, the formate is considered to be unidentate or bidentate, respectively. When it is as large as that of a free ion, it is assigned to be of bridge type. Discrimination of three different formates on the oxide surfaces is possible when at least two types of formates are observed on those surfaces.

On MgO unidentate formate was produced at low temperatures, and then bidentate (minor) and bridge (major) formates were produced with increasing temperature. The unidentate formate was preferably transformed to the bridge formate in the presence of water vapor. Thus, the bridge formate was the main species under the catalytic WGS reaction conditions on MgO.

It was found that the bridge formate produced from an OH group (H$_2$O) and CO was never converted to the products, H$_2$ and CO$_2$, in vacuum, whereas the formate has been positioned as a reaction intermediate for the catalytic WGS reaction.[11] To clarify the reason of the difference in behavior of the surface formate under vacuum and in the working state, decomposition of the surface formate was examined. Table 1 shows the rate constants, k_+ and k_-, for the *forward* decomposition of the surface formate to form H$_2$ + CO$_2$ and *backward* decomposition of the surface formate to form H$_2$O + CO, respectively, without and with water vapor (0.67 kPa).[11]

$$H_2O + CO \underset{\text{backward decomposition}}{\overset{\text{formate formation}}{\rightleftharpoons}}$$
$$HCOO^-(a) + H^+(a) \xrightarrow{\text{forward decomposition}} H_2 + CO_2$$

Note that k_+ for the *forward* decomposition of the formate to produce H$_2$ + CO$_2$ was zero in vacuum, whereas in the presence of gas phase water, the formation of H$_2$ and CO$_2$ was observed. The *backward* decomposition of the formate to H$_2$O + CO was markedly suppressed, and the *forward* decomposition path was opened, by coexistence of water vapor. The change of the selectivity of the formate decomposition is not due to a thermodynamical shift because the total quantity of OH groups and adsorbed water increased only 2−3 times by the presence of gas phase water compared to that in vacuum, while a drastic change in selectivity occurred by the ambient water

(9) Shido, T.; Asakura, K.; Iwasawa, Y. *J. Chem. Soc., Faraday Trans. 1* **1989**, *85*, 441.
(10) Nakamoto, K. *Infrared and Raman Spectra of Inorganic and Coordination Compounds*, 3rd ed.; Wiley: New York, 1987.
(11) Shido, T.; Asakura, K.; Iwasawa, Y. *J. Catal.* **1990**, *122*, 55.

Scheme 2. Water—Gas Shift Reactions Promoted by Coexistence of H₂O on MgO (a) and ZnO (b)
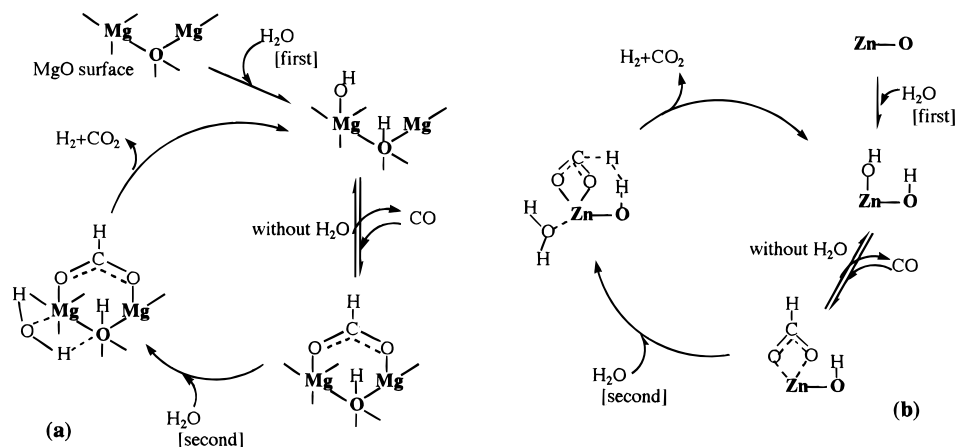
as shown in Table 1. Rather, the decomposition is kinetically controlled, where gas phase water molecules induce the dehydrogenation path of the surface formate to form CO_2 and H_2.

The surface formate was stabilized by coadsorbed water as revealed by an upshift of the TPD peak, suggesting interaction of the formate with the coadsorbed water. Table 1 shows $\nu(CD)$, $\nu_{as}(OCO)$, and $\nu_s(OCO)$ bands for $DCOO^-$ formed on a deuterium-labeled MgO surface and the rate constants of the *forward* and *backward* decompositions of the deuterium-labeled formates under the ambient methanol, pyridine, and THF, besides water.[11] The $\nu_{as}(OCO)$ and $\nu_s(OCO)$ peaks were observed to shift in the presence of the electron-donating molecules. The formate anion cannot directly interact with the electron donors because of the repulsive force between the anion and the donor. Among the electron donors water and methanol promoted the *forward* decomposition of the formate to H_2 and CO_2, while pyridine and THF gave no effect on the reactivity of the formate. It is most likely that the electron-donating molecules adsorb on coordinatively unsaturated Mg cations on which the formates also adsorb. Water and methanol molecules can also have hydrogen bonding with the lone pair electron of the lattice oxygen atom adjacent to the Mg cation to withdraw the electrons from the oxygen atom. It has been demonstrated that the energy level of the 3s orbital of Mg increases by coordination of the water hydrogen to the lattice oxygen. The change of the level structure would make chemical bondings between the Mg atoms and the formate oxygen atoms stronger, and result in a change of the selectivity of the formate decomposition.

All of the surface formates formed from H_2O and CO decompose *backwardly* to H_2O and CO under vacuum, whereas the majority of the formates decompose *forwardly* to H_2 and CO_2 under the ambient H_2O. The mechanism for the catalytic WGS reaction (reactant-promoted mechanism) on MgO is illustrated in Scheme 2a. The electron-donating and -withdrawing interaction of a water molecule with the Mg—O pair site is a key issue for the *forward* decomposition of the bridge formate to produce H_2 and CO_2. At a reaction temperature of 600 K the coadsorbed water molecules can exist only under the ambient water, and hence the surface reaction is successively assisted by the gas phase molecule.

WGS Reaction on the ZnO Surface. The $\nu(OD)$ peak at 2706 cm^{-1} on an OD-covered ZnO surface, attributable to linear OD groups on two-coordinated Zn ions,[12] decreased by reaction with CO at 473 K accompanied with the appearance of $\nu_{as}(OCO)$ and $\nu_s(OCO)$ peaks for surface bidentate formates ($DCOO^-$) at 1568 and 1342 cm^{-1}, respectively, suggesting that the OD groups reacted with CO to produce the bidentate formates. The formates ($DCOO^-$) reacted with the D atoms of bridge (2682 cm^{-1}) or 3-fold-hollow (2669 cm^{-1}) OD groups at 573 K as monitored by FT-IR,[12] evolving D_2, CO_2, D_2O, and CO in the gas phase.

It was found that the rate constant of the *forward* decomposition of the surface bidentate formate ($DCOO^-$) to produce D_2 and CO_2 increased from 0.34×10^{-4} s^{-1} under vacuum to 5.3×10^{-4} s^{-1} under the ambient water. Electron donors such as NH_3, CH_3OH, pyridine, and THF also increased the decomposition rate; the rate constants of the *forward* decomposition of the surface formates at 553 K were determined to be 28.0×10^{-4}, 7.7×10^{-4}, 8.1×10^{-4}, and 6.0×10^{-4} s^{-1} under NH_3, methanol, pyridine, and THF vapors (0.4 kPa), respectively. It is likely the driving force for the *forward* decomposition of the formate is electron donation of the adsorbed molecule to the Zn ion on which the bidentate formate adsorbs. The reactant-promoted mechanism for the catalytic WGS reaction on ZnO is illustrated in Scheme 2b. The manifestations of the activation of formate are different from those observed with MgO in Scheme 2a probably because the surface structure of the oxide catalysts and the type of the formates are different between MgO and ZnO.

The catalytic WGS reaction on ZnO may proceed as follows. The first water molecule dissociates at mainly the Zn_{2c}—O_{3c} pair to form a linear OH group and a bridge or 3-fold-hollow OH group. The linear OH group on Zn reacts with CO to produce the bidentate formate through unidentate formate. Seventy percent of the formates *backwardly* decompose to the original H_2O and CO under vacuum, and only 30% of them *forwardly* decompose to react with the bridge or 3-fold-hollow OH groups to produce H_2 and CO_2. In the presence of gas phase water, the weakly adsorbed (second) water molecule adsorbs on the Zn atom and enhances the *forward* decomposition,

(12) Shido, T.; Iwasawa, Y. *J. Catal.* **1991**, *129*, 343.

catalyst	react temp/K	gas phase	$k_+ + k_-$/s^{-1}	k_+/k_-/ (%/%)	$E_a(k_+)$/ (kJ mol^{-1})
ZnO	533	vacuum	1.3×10^{-4}	26/74	155
		D_2O	5.3×10^{-4}	100/0	109
Rh/CeO$_2$	443	vacuum	1.1×10^{-5}	35/65	56
		D_2O	1.1×10^{-3}	100/0	33

^{a} k_+ = rate constant for $DCOO^- + D^+ \rightarrow D_2 + CO_2$; k_- = rate constant for $DCOO^- + D^+ \rightarrow D_2O + CO$; $E_a(k_+)$ = activation energy for the forward decomposition; $E_a(k_-)$ = activation energy for the backward decomposition.

where almost 100% of the formates decompose to H_2 and CO_2.[12] The activation energy for the *forward* decomposition of the formate decreases from 155 kJ mol^{-1} under vacuum to 109 kJ mol^{-1} under the ambient water as shown in Table 2.[12]

The WGS reaction is a reversible reaction; that is, the WGS reaction attains equilibrium with the reverse WGS reaction. Thus, the fact that the WGS reaction is promoted by H_2O (a reactant), in turn, implies that the reverse WGS reaction may also be promoted by a reactant, H_2 or CO_2. In fact the decomposition of the surface formates produced from $H_2 + CO_2$ was promoted 8−10 times by gas phase hydrogen. The WGS and reverse WGS reactions conceivably proceed on different formate sites of the ZnO surface unlike usual catalytic reaction kinetics, while the occurrence of the reactant-promoted reactions does not violate the principle of microscopic reversibility. The activation energy for the decomposition of the formates (produced from $H_2O + CO$) in vacuum was 155 kJ mol^{-1}, and the activation energy for the decomposition of the formates (produced from $H_2 + CO_2$) in vacuum was 171 kJ mol^{-1}. The selectivity for the decomposition of the formates produced from $H_2O + CO$ at 533 K was 74% for $H_2O + CO$ and 26% for $H_2 + CO_2$, while the selectivity for the decomposition of the formates produced from $H_2 + CO_2$ at 533 K was 71% for $H_2 + CO_2$ and 29% for $H_2O + CO$[13] as follows:
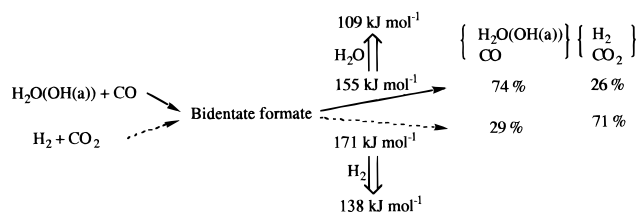
The drastic difference in selectivity is not presently understood. It is clear, however, that it should not be ascribed to the difference of the bonding feature in the zinc formate species because of almost the same frequencies of $\nu(CH)$, $\nu_{as}(OCO)$, and $\nu_s(OCO)$ for both bidentate formates produced from $H_2O + CO$ and $H_2 + CO_2$. Note that the origin ($H_2O + CO$ or $H_2 + CO_2$) from which the formate is produced is "remembered" as a main decomposition path under vacuum, while the origin is "forgotten" by coadsorbed H_2O.

In the reverse WGS reaction hydrogen promoted both decomposition paths of the formate to $H_2 + CO_2$ and H_2O

+ CO, and the decomposition selectivity did not change. Thus, the mechanism of promotion of hydrogen is different from that of electron donors in the WGS reaction. CO_2 not only blocked the adsorption sites of H_2 but also suppressed the decomposition of the formate intermediate. The rate constant for the steady-state reaction was larger than the rate constant obtained from the formate decomposition in vacuum, but it was smaller than that for the formate decomposition under the ambient H_2. As a result, the reverse WGS reaction proceeds with a balance of the H_2 promotion and the CO_2 suppression.[13]

WGS Reaction on the Rh/CeO$_2$ Surface. CeO$_2$ was contrasted with MgO and ZnO; the surface formate on CeO$_2$ was stabilized by coexistence of water vapor, where the selectivity to H_2 and CO_2 only increased as a result of suppression of the *backward* decomposition of formate more than that of the *forward* decomposition by water vapor. We have tried to modify the properties of the CeO$_2$ surface by doping a small amount (0.2 wt %) of Rh to CeO$_2$[14] as Rh catalysts with CeO$_2$ have been used as automobile exhaust catalysts,[15] on which the WGS reaction proceeds.

Surface formates on both Rh/CeO$_2$ and CeO$_2$ surfaces were of the bidentate type. The bidentate formate was produced and decomposed more easily on Rh/CeO$_2$ than on CeO$_2$. The activation energy of the *forward* decomposition of the formate on Rh/CeO$_2$, 56 kJ mol^{-1}, was much lower than 207 kJ mol^{-1} for CeO$_2$.

In the catalytic WGS reaction on Rh/CeO$_2$, linear OH groups reacted with CO to produce the bidentate formates. In vacuum, 65% of the surface formates decomposed *backwardly* to $H_2O + CO$ and 35% of them decomposed *forwardly* to $H_2 + CO_2$. When water vapor coexisted, 100% of the formates decomposed *forwardly* to $H_2 + CO_2$ as shown in Table 2. The activation energy for the *forward* decomposition of the formate decreased from 56 kJ mol^{-1} in vacuum to 33 kJ mol^{-1} by the presence of water vapor. By addition of a small amount of Rh (0.2 wt %) to CeO$_2$, the rate of the WGS reaction increased tremendously as shown in Table 2, and the value of the *forward* decomposition rate constant (k_+) was promoted about 100 times by coexistence of gas phase water.[14]

The isotope effect was observed with the hydrogen atom of the formate and not observed with the hydrogen atom of the water molecule. The result is similar to that observed on ZnO, where the rate-determining step of the formate decomposition is suggested to be dissociation of the CH bond of the bidentate formate. In summary, the reaction mechanism for the catalytic WGS reaction on Rh/CeO$_2$ is essentially the same as that on ZnO.

Prospective

Examples of surface reactions assisted by gas phase molecules are not to be restricted to the particular cases mentioned above, but the surface phenomenon promoted by the ambient gas may be extended to many catalytic systems. It has also been reported that the reactivity of the formate on Ni/SiO$_2$ catalyst was markedly increased by the presence of formic acid in the ambient gas

(13) Shido, T.; Iwasawa, Y. *J. Catal.* **1993**, *140*, 575.

(14) Shido, T.; Iwasawa, Y. *J. Catal.* **1993**, *141*, 71.
(15) Wei, J. *Adv. Catal.* **1975**, *24*, 57.

compared to that at the same coverage under vacuum, where the interaction between the molecules in the vapor phase and the surface formate is proposed to be the rate-determining step.[16]

Xu et al. recently reported that bulk lattice oxygen species on Na_2WO_3/CeO_2 catalyst do not participate directly in the oxidative coupling of methane, but the active oxygen species involved in the activation of methane exist only in the presence of gas phase oxygen.[17] Au and Roberts reported the promotion of surface-catalyzed reactions by gaseous additives.[18] They observed that the surface oxygen transient generated during the dissociative chemisorption of the coadsorbed promoter molecules such as O_2, NO, and N_2O on Mg(0001) was active for H abstraction of NH_3, while the chemisorbed oxygen overlayer was relatively unreactive. These examples represent the active oxygen transient present under the ambient O_2 as the key issue of the surface reactions. Sasaki et al. found a remarkable enhancement of the NH_3 decomposition on Ru(001) by coexistence of CO which is not involved in the reaction.[19,20] Similarly, Burke and Madix demonstrated that the introduction of CO onto the surface presaturated with hydrogen and ethene brought about the

formation of ethane, a reaction which did not occur in the absence of CO.[21] Rodrigues et al. observed a promotional effect of CO on the growth of filamentous carbon from ethene.[22] Exposure of a Fe catalyst to a $C_2H_4-H_2$ mixture at 873 K resulted in only minor decomposition of the ethene; however, upon addition of a small amount of CO to the system, there was a dramatic increase in the amount of filamentous carbon formed. These examples may be categorized in a different class of surface catalytic/stoichiometric reactions assisted by gas phase molecules, where the phenomena involve strong adsorption of gas phase molecules.

As described in sections 2 and 3, *weakly adsorbed molecules which can exist only under catalytic reaction conditions play an important role in surface catalytic reactions even if the adsorption of the "promoter" is very weak or is undetectable*. Surface intermediates under the ambient gas molecules behave in a different way from those under vacuum, showing rate enhancement and selectivity change of the surface reaction in the presence of ambient gas. On the basis of the concept of surface catalytic reactions assisted by gas phase molecules, one may design new catalytic systems through in situ activation of inactive or stable surface sites under the conditions of a target reaction.[1,23]

AR950141J

(16) Takahashi, K.; Miyamoto, E.; Shoji, K.; Tamaru, K. *Catal. Lett.* **1988**, *1*, 213.

(17) Xu, Z.; Yang, X.; Lunsford, J. H.; Rosynek, M. P. *J. Catal.* **1995**, *154*, 163.

(18) Au, C.-T.; Roberts, M. W. *J. Chem. Soc., Faraday Trans. 1* **1987**, *83*, 2047.

(19) Sasaki, T.; Aruga, T.; Kuroda, H.; Iwasawa, Y. *Surf. Sci. Lett.* **1989**, *224*, L969.

(20) Sasaki, T.; Aruga, T.; Kuroda, H.; Iwasawa, Y. *Surf. Sci.* **1990**, *240*, 223.

(21) Burke, M. L.; Madix, R. J. *J. Am. Chem. Soc.* **1991**, *113*, 3675.

(22) Rodrigues, N. M.; Kim, M. S.; Baker, R. T. K. *J. Catal.* **1993**, *144*, 93.

(23) Iwasawa, Y. *Catal. Today* **1993**, *18*, 21.